Proceedings of the
Annual Stability Conference
Structural Stability Research Council
San Antonio, Texas, March 21-24, 2017

Analysis of Rectangular CFT Columns Subjected to Elevated Temperature

Zhichao Lai[1], Amit H. Varma[2], and Anil Agarwal[3]

Abstract
The current AISC Specification (AISC 360-10) does not specify design equations for estimating the axial compressive strength of concrete-filled steel tube (CFT) columns subjected to elevated temperature. This paper uses a fiber-based analytical approach, which was developed and benchmarked previously by the authors, to investigate the effects of various parameters on the behavior and strength of rectangular CFT columns subjected to elevated temperature. The parameters considered were the steel tube yield stress (F_y), concrete compressive strength (f'_c), tube width-to-thickness ratio (B/t), column slenderness ratio (KL/r), and magnitude of temperature. Results from the parametric studies indicate that the axial compressive strength of rectangular CFT columns decreases significantly with increasing temperature. Increasing the concrete compressive strength (f'_c) can effectively improve the axial compressive strength of rectangular CFT columns subjected to elevated temperature. While changing the steel tube yield stress (F_y) or the steel tube width-to-thickness ratio (B/t) have smaller influences.

1. Introduction

CFT members consist of rectangular or circular steel tubes filled with concrete. The presence of the concrete infill improves the strength, stiffness, and fire resistance of these composite members as compared to hollow steel tube members. As an innovative and efficient structural component, CFT members have been used widely around the world in various types of structures including composite bridges, composite moment or braced frames, piles, and transmission towers, etc.

Significant experimental tests have been conducted to investigate the strength and behavior of CFT columns. These have been summarized independently by Nishiyama et al. (2002), Kim (2005), Gourley et al. (2008), Hajjar et al. (2013), Lai et al. (2014a) and Lai and Varma (2015) among others. These experimental tests indicate that the behavior and strength of CFT columns depend on parameters such as the tube slenderness ratio (width-to-thickness ratio b/t), steel yield stress (F_y), concrete compressive strength (f'_c), and member length. For rectangular CFT

[1] Ph.D., Postdoctoral research engineer, Purdue University, Lyles School of Civil Eng., West Lafayette, IN. <laiz@purdue.edu>
[2] Professor, Purdue University, Lyles School of Civil Eng., West Lafayette, IN. < ahvarma@purdue.edu >
[3] Assistant Professor, Department of Civil Eng., Indian Institute of Technology Hyderabad, Telangana, India, <anil@iith.ac.in>

columns, the governing failure mode usually involves local buckling of the steel tube and limited confinement of the concrete infill. For circular CFT columns, the failure mode usually involves both the steel tube and concrete infill reaching their individual material strengths (yielding and crushing). However, the longitudinal (axial) stress capacity of the materials is influenced by the transverse interaction between the steel tube and concrete infill, which leads to the hoop stresses (transverse tensile) in the steel tube wall and confinement to the concrete infill (Lai and Varma 2016).

Significant experimental tests have also been conducted to investigate the fire behavior of CFT columns. For example, researchers from Canada (Lie and Carson 1988, Lie 1994, Kodur and Lie 1996) tested 17 circular CFT columns subjected to combined constant axial load and ASTM E119 (2016) standard fire loading. The test parameters included the concrete infill type (plain, bar-reinforced, or fiber-reinforced), diameter of the steel tube (141-406 mm), thickness of the steel tube (4.8 to 12.7 mm), and axial load ratio (0.1-0.6). Experimental results indicated that: (i) CFT columns with bar-reinforced or fiber-reinforcement concrete had higher FRR than those with plain concrete, and (ii) the FRR decreased with increasing axial load ratio.

Researchers from Japan (Sakumoto et al. 1994) conducted standard ASTM E119 (2016) fire tests on 18 rectangular CFT columns. The test parameters were the axial load ratio (0.2 or 0.3), eccentricity (0 or 30 mm), fire protection type (ceramic or intumescent), steel type (fire-resistant or conventional). The tests showed that CFT columns with fire protection had significant higher fire resistant rating (FRR) (about 2 hours) than those without fire protections (30 mins). The FRR values decreased with increasing axial load ratio or eccentricity. For specimens with fire protection, the protection type and steel type had no obvious influence on the FRR.

Researchers from the US (Varma et al. 2013) tested 13 rectangular CFT beam-columns subjected to combined: (i) constant axial load, (ii) bending moment, and (iii) ASTM E119 (2016) standard fire loading. The test parameters were the steel tube diameter (254 or 305 mm), steel tube thickness (6.4, 8.0, or 9.5 mm), concrete compressive strength (48 or 69 MPa), axial load ratio (0.15 or 0.3), and hours of loading (0, 1, or 2 hours). The tests indicated that the moment capacity and flexural stiffness decreased with increasing steel surface temperature. The other parameters had a small influence on the moment capacity and flexural stiffness.

Researchers from China (Han et al. 2003) have also conducted experimental tests on 11 CFT columns subjected to combined constant axial load and ISO-834 (1975) fire loading. The parameters considered were the tube depth-to-width ratio (1.0, 1.5 or 2.0), tube slenderness ratio (37.5 to 45.5), eccentricity (0, 45, or 105 mm), and protection thickness (0 to 22.6 mm). The tests showed that: (i) FRR of CFT columns decreased significantly with decreasing protection thickness, and (ii) eccentricity had a moderate effect on the FRR of CFT columns without fire protection.

Several analytical studies have also been conducted to investigate the fire behavior of CFT columns. These include fiber-based analytical approach (Lie 1994, Kodur and Lie 1996, Han 2001, Han et al. 2003, and Hong and Varma 2010) and detailed 3D finite element approach (Hong and Varma 2009). Detailed 3D finite element approach can explicitly account for complexities such as steel tube local buckling, concrete cracking, interactions between the steel

tube and concrete confinement (which results in the steel tube hoop stress and concrete confinement), and moisture evaporation (Hong and Varma 2009). However, they are time-consuming for conducting parametric studies. Fiber-based analysis approach can implicitly account for steel tube local buckling, concrete cracking, and the interactions between the steel tube and concrete infill. However, it cannot account for the moisture evaporation. This may result in slightly higher (conservative) estimation of the concrete temperature inside the CFT cross-sections (Hong and Varma 2009).

These existing experimental and analytical investigations usually focus on determining the FRR value of CFT columns. Results from these investigations cannot be directly used to estimate the axial compressive strength of CFT columns subjected to elevated temperature. This paper used a fiber-based analytical approach, which was developed and benchmarked previously by the authors, to investigate the effects of various parameters on the behavior and strength of rectangular CFT columns subjected to elevated temperature. The parameters considered were the steel tube yield stress (F_y), concrete compressive strength (f'_c), tube width-to-thickness ratio (B/t), column slenderness ratio (KL/r), and magnitude of temperature.

2. Background

Previous research (Hong and Varma 2010) developed and benchmarked a fiber-based analytical approach for predicting the behavior of CFT columns subjected to combined constant axial load and standard fire loading. The approach consists of three parts: (i) two-dimensional heat transfer (2D HT) analysis, (ii) section moment-curvature ($M-\phi$) analysis, and (iii) nonlinear column inelastic buckling (NICB) analysis. As the heating time (t) increases, the 2D HT analysis calculates the temperature distribution of a CFT column cross-section at each time increment t. The $M-\phi$ analysis then calculates the moment-curvature response of the CFT column cross-section subjected to (i) the constant axial load (P) and (ii) the temperature distributions calculated from the 2D HT analysis. After that, the NICB analysis calculates the deflection of the CFT column at time t and determines whether the column fails or not. The column failure is assumed to occur when the calculated external moment at any section along the length (typically at mid-height) has become greater than the section moment capacity obtained from the $M-\phi$ analysis.

Therefore, this approach provides the following results for CFT columns: (i) fire resistance rating (FRR) values, (ii) temperature-dependent $M-\phi$ curves, (iii) axial displacement-time responses, and (iv) lateral deflection-time responses. In this current research, the original Huang and Varma's approach was modified to calculate the strength of rectangular CFT columns subjected to elevated temperature. The modified approach is essentially the same as the original Huang and Varma's approach, except that this approach monotonically increases the axial load until failure occurs. While in the original approach, the heating time (temperature) is increased monotonically until failure occurs.

In the modified approach (referred as the HT-NICB approach hereafter), the 2D HT analysis first calculates the temperature distribution of a CFT column cross-section at desired steel tube surface temperature T. Fig. 1 shows an example of the temperature distribution of a CFT column subjected to 30-min ASTM E119 (2016) standard fire loading. The geometric and material properties of this specimen is the same as that of Specimen CFT-12-34-15-7-2h tested by Varma

et al. (2013). These details will also be explained in the next section. Then, at each axial load increment, the $M-\phi$ analysis calculates the moment-curvature response of the CFT column cross-section subjected to the temperature distributions calculated from the 2D HT analysis. Fig. 2 shows the moment-curvature response of Specimen CFT-12-34-15-7-2h subjected to pure bending and elevated temperature. Finally, the NICB analysis calculates the deflection of the CFT column at each axial load level and determines whether the column fails or not.

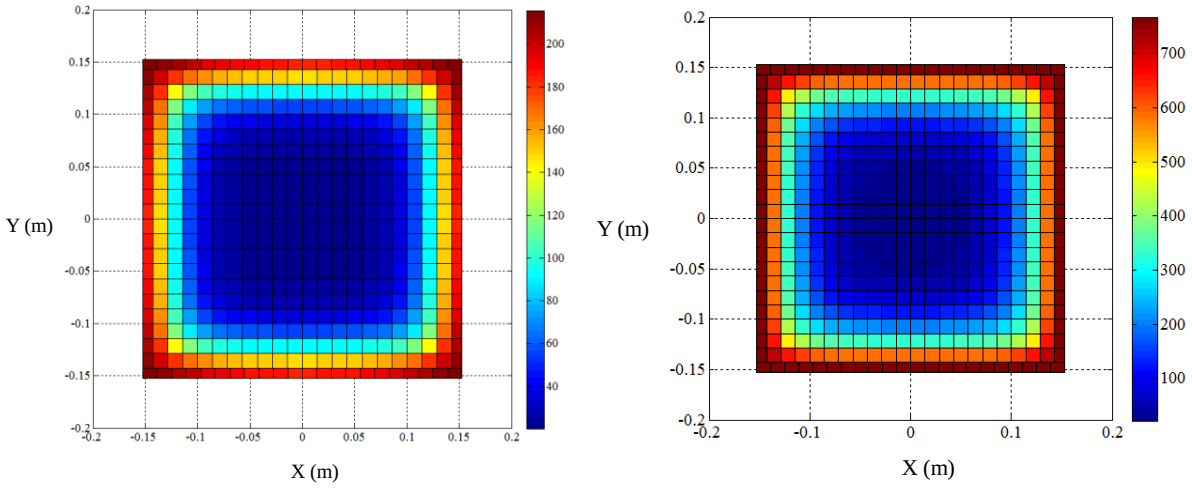

Figure 1: Temperature distribution (in ºC) of Specimen CFT-12-34-15-7-2h subjected to 30-min ASTM E119 standard fire loading: (a) with 6.4 mm thick gypsum plaster as fire protection and (b) without any fire protection

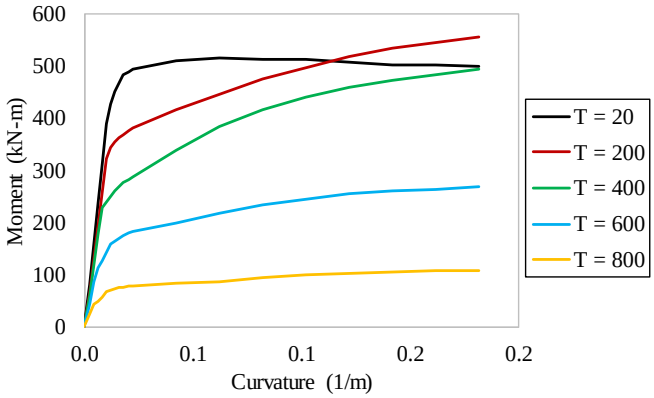

Figure 2: Effect of temperature (in ºC) on the moment-curvature response of Specimen CFT-12-34-15-7-2h subjected to pure bending

3. Parametric studies

As discussed previously, the strength of CFT columns subjected to elevated temperature was influenced by 10 parameters, which include: (1) steel tube yield stress (F_y), (2) concrete compressive strength (f'_c), (3) tube width-to-thickness ratio (B/t), (4) column slenderness ratio (KL/r), (5) magnitude of temperature, (6) tube width-to-depth ratio (B/H), (7) cross-section type (rectangular or circular), (8) fire protection, (9) steel type (fire-resistant or conventional), and (10) concrete infill type (plain, bar-reinforced or fiber-reinforce). This paper focuses on evaluating the effects of the first five parameters. Therefore, only square CFT columns made from conventional steel and plain concrete and without any fire protection were considered.

Specimen CFT-12-34-15-7-2h tested by Varma et al. (2013) was selected as the prototype specimen. This specimen was made of conventional steel (F_y = 351 MPa) and filled with plain concrete (f'_c = 48 MPa). This specimen had a length (L) of 1.65 m, steel tube width (B) of 305 mm, steel tube thickness (t) of 9.5 mm, and 6.4 mm thick gypsum plaster as fire protection cover. However, the fire protection was not included in the parametric studies in the current research.

Three groups of parametric analyses (280 analyses in total) were conducted on the prototype column by (i) varying the magnitude of each of the first three parameters in the corresponding analysis group and (ii) varying the 4th (i.e., the column slenderness ratio KL/r) and 5th (i.e., the temperature magnitude) parameters in every analysis group. For example, the effect of steel tube yield stress was investigated in the first analysis group by (i) varying the steel tube yield stress (F_y) while keeping the other three parameters the same as that of the prototype member and (ii) varying the column slenderness ratio (KL/r) and temperature magnitude. The column slenderness ratio (KL/r) was varied by changing member length (L). Eight different member length-to-depth ratios (3.0, 6.0, 10.0, 15.0, 20.0, 25.0, 30.0 and 40.0) were used in each analysis group. The radius of gyration r is calculated as $\sqrt{(I_s + I_c)/(A_s + A_c)}$, where I_s is the moment of inertia of the steel tube, I_c is the moment of inertia of the concrete infill, A_s is the cross-section area of the steel tube, and A_c is the cross-section area of the concrete infill, respectively. Five steel tube surface temperatures were used in each analysis group, i.e., 20 ^{o}C (which represents ambient temperature), 200 ^{o}C, 400 ^{o}C, 600 ^{o}C, and 800 ^{o}C. Table 1 summarizes details of members used in the parametric studies.

Table 1: Analysis Matrix

Group No.	F_y (MPa)	f'_c (MPa)	B (mm)	t (mm)	H (mm)	B/t
1	525	48	305.0	9.50	305.0	32
	421	48	305.0	9.50	305.0	32
	351	48	305.0	9.50	305.0	32
2	351	70	305.0	9.50	305.0	32
	351	21	305.0	9.50	305.0	32
3	351	48	305.0	6.35	305.0	48
	351	48	305.0	4.77	305.0	64

All of the parametric analyses assumed: (i) full bond between the steel tube and concrete infill, (ii) geometric imperfections with sinusoidal shape and magnitude equal to L/7500, and (iii) no steel tube local buckling. These assumptions were considered reasonable based on the sensitivity analyses conducted by Hong and Varma (2009).

3.1 Effect of the steel tube yield stress (F_y)

Three steel tube yield stress values were used in the first analysis group, i.e., 358 MPa, 421 MPa, and 525 MPa. This resulted in a total of 120 analyses in this group. The yield stress was limited to 525 MPa because it is the maximum yield stress allowed for steel tubes by AISC 360-10 (2010). Fig. 3 shows the effect of temperature on the column curves. As shown, the axial

compressive strength of CFT columns decreases as the steel tube surface temperature increases. The effect of temperature is more significant for columns with intermediate length and less significant for short and slender columns. For example, as the steel tube surface temperature increased from 20 to 200 ºC, the axial strength decreased 13%, 47%, and 36% for columns with F_y of 358 MPa and KL/r ratio of 10.4, 69.3, and 138.6, respectively. Fig. 4 shows the effect of steel tube yield stress (F_y). As shown, the axial compressive strength of CFT columns increases with increasing steel tube yield stress. However, the effect is less significant as the steel tube surface temperature increases. This is because the strength of steel tube decreases significantly as the temperature increases.

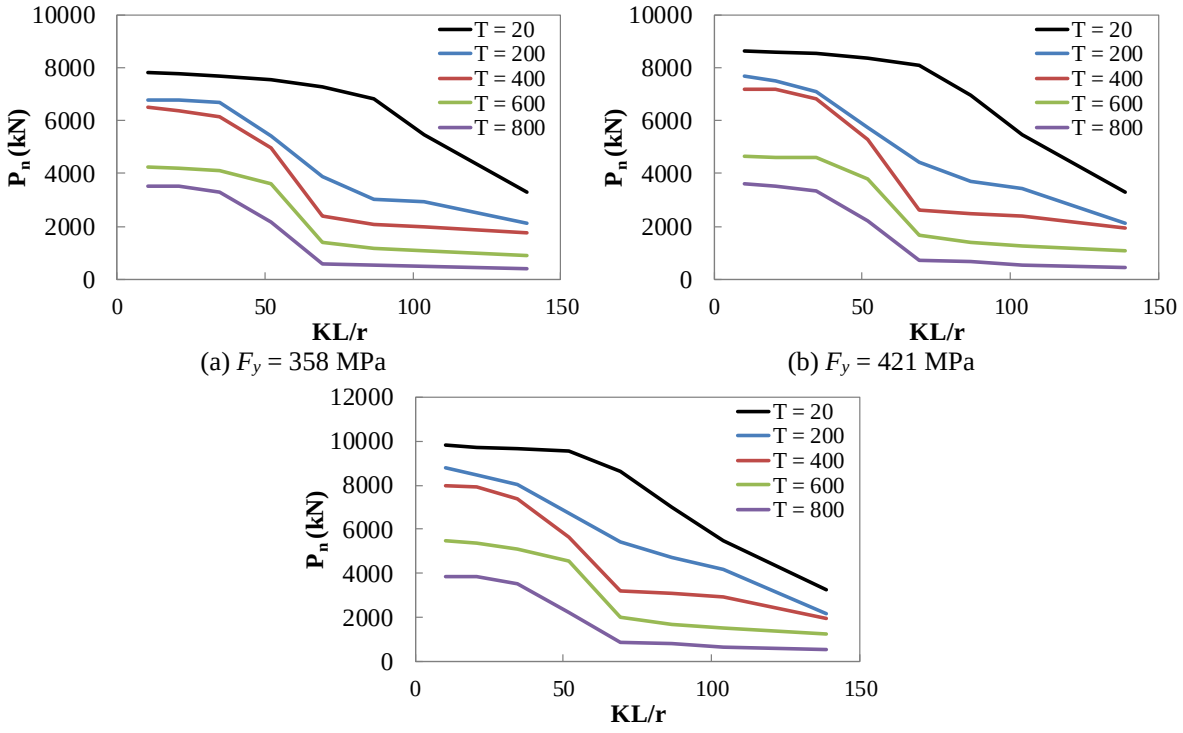

(a) F_y = 358 MPa (b) F_y = 421 MPa

(c) F_y = 525 MPa

Figure 3: Effect of temperature (in ºC) on the columns curves of rectangular CFT members with different steel tube yield stress (F_y)

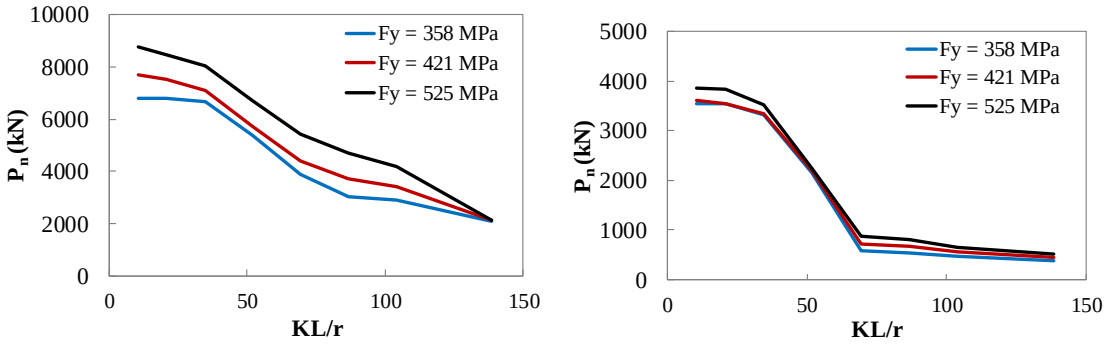

(a) T = 200 ºC (b) T = 800 ºC

Figure 4: Effect of steel tube yield stress (F_y) on the columns curves of rectangular CFT members subjected to elevated temperature

3.2 Effect of concrete compressive strength (f'_c)

Three concrete compressive strength values were used in the second analysis group, i.e., 21 MPa, 48 MPa, and 70 MPa. CFT members with the concrete compressive strength of 48 MPa have been analyzed in the first analysis group. Therefore, 80 additional analyses were conducted in the second analysis group. The concrete compressive strength was limited to 70 MPa because it is the maximum compressive strength allowed for concrete infill by AISC 360-10 (2010). Fig. 5 shows the effect of temperature on the column curves. Similar to Fig. 3, this figure indicates that: (i) the axial compressive strength of CFT columns decreases as the steel tube surface temperature increases, and (ii) the effect of temperature is more significant for columns with intermediate length and less significant for short and slender columns. Fig. 6 shows the effect of concrete compressive strength (f'_c). As shown, the axial compressive strength of CFT columns subjected to elevated temperature increases with increasing concrete compressive strength.

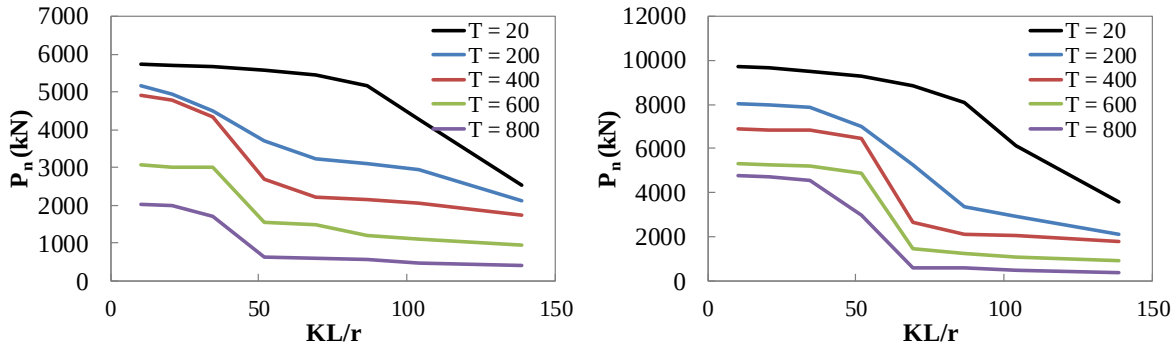

(a) f'_c = 21 MPa (b) f'_c = 70 MPa

Figure 5: Effect of temperature (in ºC) on the columns curves of rectangular CFT members with different concrete compressive strength (f'_c)

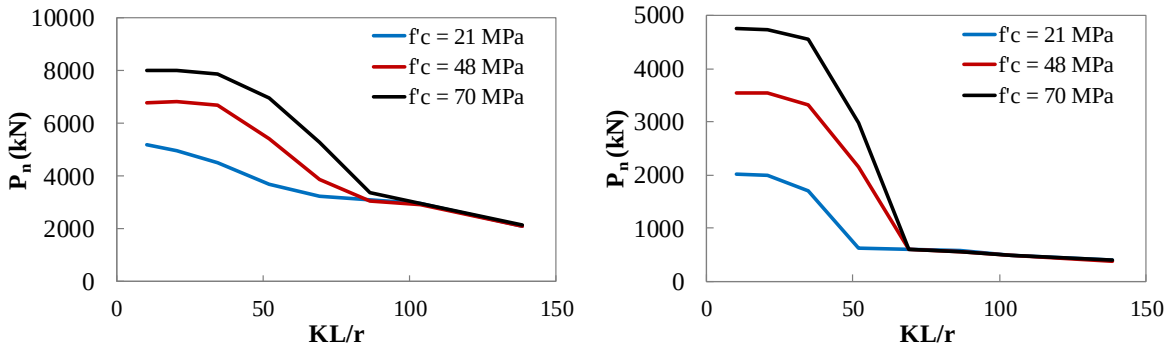

(a) T = 200 ºC (b) T = 800 ºC

Figure 6: Effect of concrete compressive strength (f'_c) on the columns curves of rectangular CFT members subjected to elevated temperature

3.3 Effect of with-to-thickness ratio (B/t)

Three steel tube width-to-thickness ratios were used in the second analysis group, i.e., 32, 48, and 64. CFT members with the width-to-thickness ratio of 32 have been analyzed in the first analysis group. Therefore, 80 additional analyses were conducted in the third analysis group. The width-to-thickness ratio was varied by changing the steel tube thickness (t) while keeping the tube width (B) constant. Fig. 7 shows the effect of temperature on the column curves. Similar to Figs. 3 and 5, this figure indicates that: (i) the axial compressive strength of CFT columns

decreases with increasing steel tube surface temperature, and (ii) the effect of temperature is more significant for columns with intermediate length. Fig. 8 shows the effect of steel tube width-to-thickness ratio (*B*/*t*). As shown, the axial compressive strength of CFT columns decreases with increasing steel tube width-to-thickness ratio. However, the effect is less significant as the steel tube surface temperature increases. This is because (i) the strength of steel tube decreases significantly as the temperature increases, and (ii) the contribution of concrete to the overall strength increases as *B*/*t* increases.

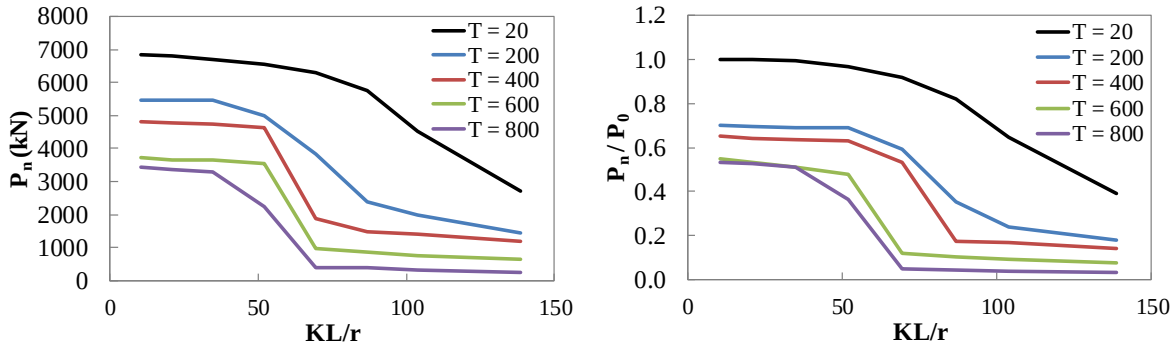

(a) *B*/*t* = 48 (b) *B*/*t* = 64

Figure 7: Effect of temperature (in ºC) on the columns curves of rectangular CFT members with different tube width-to-thickness ratios (*B*/*t*)

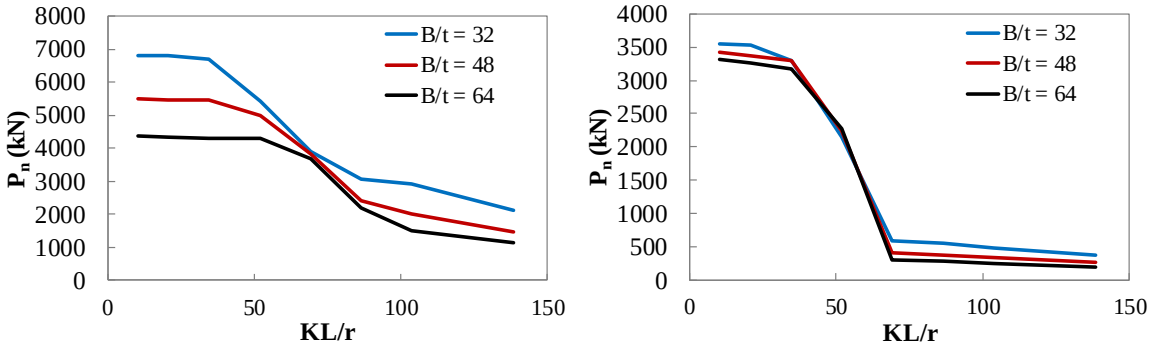

(a) *T* = 200 ºC (b) *T* = 800 ºC

Figure 8: Effect of tube width-to-thickness ratio (*B*/*t*) on the columns curves of rectangular CFT members subjected to elevated temperature

4. Future work

This paper evaluated the effects of the following five parameters on the axial compressive strength of rectangular CFT columns subjected to elevated temperature: (1) steel tube yield stress (F_y), (2) concrete compressive strength (f'_c), (3) tube width-to-thickness ratio (*B*/*t*), (4) column slenderness ratio (*KL*/*r*), (5) magnitude of temperature. However, the effects of several other parameters were not evaluated. These include: (1) tube width-to-depth ratio (*B*/*H*), (2) cross-section type (rectangular or circular), (3) fire protection, (4) steel type (fire-resistant or conventional), and (5) concrete infill type (plain, bar-reinforced or fiber-reinforce). Further investigations regarding these will be conducted using the modified HT-NICB approach. Appropriate design equations for evaluating the axial compressive strength of CFT columns subjected to elevated temperature will also be proposed using results from the current study and the further investigations.

5. Summary and conclusions

This paper used a fiber-based analytical approach, which was developed and benchmarked previously by the authors, to investigate the effects of various parameters on the behavior and strength of rectangular CFT columns subjected to elevated temperature. The parameters considered were the steel tube yield stress (F_y), concrete compressive strength (f'_c), tube width-to-thickness ratio (B/t), column slenderness ratio (KL/r), and magnitude of temperature. Results from the parametric studies indicated that the axial compressive strength of rectangular CFT columns decreased significantly with increasing temperature. The effect of temperature was more significant for columns with intermediate length and less significant for short and slender columns. Increasing the concrete compressive strength (f'_c) effectively improved the axial compressive strength of rectangular CFT columns subjected to elevated temperature. While changing the steel tube yield stress (F_y) or the steel tube width-to-thickness ratio (B/t) had smaller influences.

References

AISC 360-10. (2010). *Specification for structural steel buildings*. AISC, Chicago, IL, USA.

ASTM. (2016). *Standard test methods for fire tests of building construction and materials*. American Society for Testing and Materials, West Conshohocken, PA, USA.

Gourley, B. C., Cenk, T., Denavit, M. D., Schiller, P. H., and Hajjar, J. F. (2008). "A synopsis of studies of the monotonic and cyclic behavior of concrete-filled steel tube members, connections, and frames, Report No. NSEL-008, Department of Civil and Environmental Engineering." University of Illinois at Urbana-Champaign, Champaign, IL, USA.

Hajjar, J. F., Gourley, B. C., Tort, C., Denavit, M. D., and Schiller, P. H. (2013). "Steel-concrete composite structural systems, http://www.northeastern.edu/compositesystems." *Department of Civil and Environmental Engineering, Northeastern University*, Northeastern University.

Han, L. H. (2001). "Fire performance of concrete filled steel tubular beam-columns." *Journal of Composites for Construction*, 57(6), 695–709.

Han, L. H., Yang, Y. F., and Xu, L. (2003). "An experimental study and calculation on the fire resistance of concrete-filled SHS and RHS columns." *Journal of Constructional Steel Research*, 59(4), 427–452.

Hong, S., and Varma, A. H. (2009). "Analytical modeling of the standard fire behavior of loaded CFT columns." *Journal of Constructional Steel Research*, Elsevier Ltd, 65(1), 54–69.

Hong, S., and Varma, A. H. (2010). "Predicting fire behavior of composite CFT columns using fundamental section behavior." *Journal of ASTM International*, 7(1), 78–110.

ISO-834. (1975). *Fire resistance tests-Elements—Elements of building construction*. International Standard ISO 834, Geneva,Switzerland.

Kim, D. K. (2005). "A database for composite columns [Thesis]." Georgia Institute of Technology.

Kodur, V. K. R., and Lie, T. T. (1996). "Fire resistance of circular steel columns filled with fiber-reinforced concrete." 122(July), 776–782.

Lai, Z., and Varma, A. H. (2015). "Noncompact and slender circular CFT members: experimental database, analysis, and design." *Journal of Constructional Steel Research*, 106(3), 220–233.

Lai, Z., and Varma, A. H. (2016). "Effective stress-strain relationships for noncompact and slender CFT members." *Engineering Structures*, 124, 457–472.

Lai, Z., Varma, A. H., and Zhang, K. (2014). "Noncompact and slender rectangular CFT members: experimental database, analysis, and design." *Journal of Constructional Steel Research*, 101(10), 455–468.

Lie, T. T. (1994). "Fire resistance of circular steel columns filled with bar-reinforced concrete." *Journal of Structural Engineering*, 120(5), 1489–1509.

Lie, T. T., and Carson, S. . (1988). *Fire resistance of circular hollow steel columns filled with carbonate aggregate concrete: Test results. Internal Report No. 570*. Ottawa, Canada.

Nishiyama, I., Morino, S., Sakino, K., Nakahara, H., Fujimoto, T., Mukai, A., Inai, E., Kai, M., Tokinoya, H., Fukumoto, T., Mori, K., Yoshioka, K., Mori, O., Yonezawa, K., Uchikoshi, M., and Hayashi, Y. (2002). *Summary of research on concrete-filled structural steel tube column system carried out under the U.S.-Japan cooperative research on composite and hybrid structures*. Ibaraki Prefecture, Japan.

Sakumoto, Y., Okada, T., Yoshida, M., and Tasaka, S. (1994). "Fire resistance of concrete-filled, fire-resistant steel-tube columns." *Journal of Materials in Civil Engineering*, 6(2), 169–184.

Varma, A. H., Hong, S., and Choe, L. (2013). "Fundamental behavior of CFT beam-columns under fire loading." *Steel and Composite Structures*, 15(6), 679–703.